Mechanical design and analysis of a 40mm aperture high field Nb3Sn dipole using skin welding to apply all prestress

G. Ambrosio, Fermilab, Batavia IL USA

Abstract

The mechanical design of a 40 mm aperture 2 layer NbSn High field dipole is reported. The basic ideas are presented. The study using analytical and many FE models and.a test of different contact elements are as well reported.

INTRODUCTION

Fermilab in collaboration with LBNL and KEK is working on the design and production of dipole models for a Very Large Hadron Collider. At present the use of Nb3Sn in wind and react technique is explored. The goal is a low cost 10-11 tesla magnet operated at 4.2 K.

Up to now many different cross sections have been proposed with aperture ranging from 40 to 50 mm [1,2,3,4]. All of them have a two layer cos θ layout. Different mechanical designs are being explored, the main common characteristics are: the use of thin spacers (about 10 mm thick) instead of collars, and the use of clamp or skin welding to apply all prestress.

This report concerns the mechanical design of a 40 mm aperture with a cable made of 38 0.808mm diameter strands [3] adopting skin welding under pressure to apply all prestress.

	mm
Aperture radius	20
Width of each layer	15.4
Layer to layer insulation thickness	0.72
Ground insulation thickness	1
Spacer inner radius	52.65
Yoke inner radius	60
Yoke outer radius	200
Skin thickness	10
Gap control spacer full length	120

Table 1: Cross section dimensions.

1. MECHANICAL DESIGN

Following is a list describing the main characteristics of this design. Dimensions and materials are reported in Tables 1 and 2. A FE model of the cross section with some dimensions and nomenclature is shown in Figure 1.

- There are no collars: the poles are impregnated together with the coils in order to have a self-consisting pipe (late referred to as coil pipe). Stainless steel spacers (late referred to as coil spacers) are set between the coils and the yoke.

- The yoke has a vertical tapered gap. It is open at room temperature, closes during cooldown and remains closed at operating current.
- The coil pipe will be centered respect to the yoke by keys on the vertical plane. A small gap on the vertical plane should avoid any contact between the two coil spacers. These spacers will be centered respect to the yoke by keys on the mid-plane.
- The skin applies all prestress. Its welding is done under a press.
- Al gap control spacer will be used to avoid excessive prestress at room temperature.
- The dimensions of yoke aperture and gaps are computed in order to give a small deformation of the coil (Rx < Ry) at room temperature. This deformation increases during the cooldown since the gap closes. The magnetic forces deform the coil in the opposite direction because the highest radial component is on the mid-plane. The two effects balance at operating current keeping the coil deformation lower than few μm.

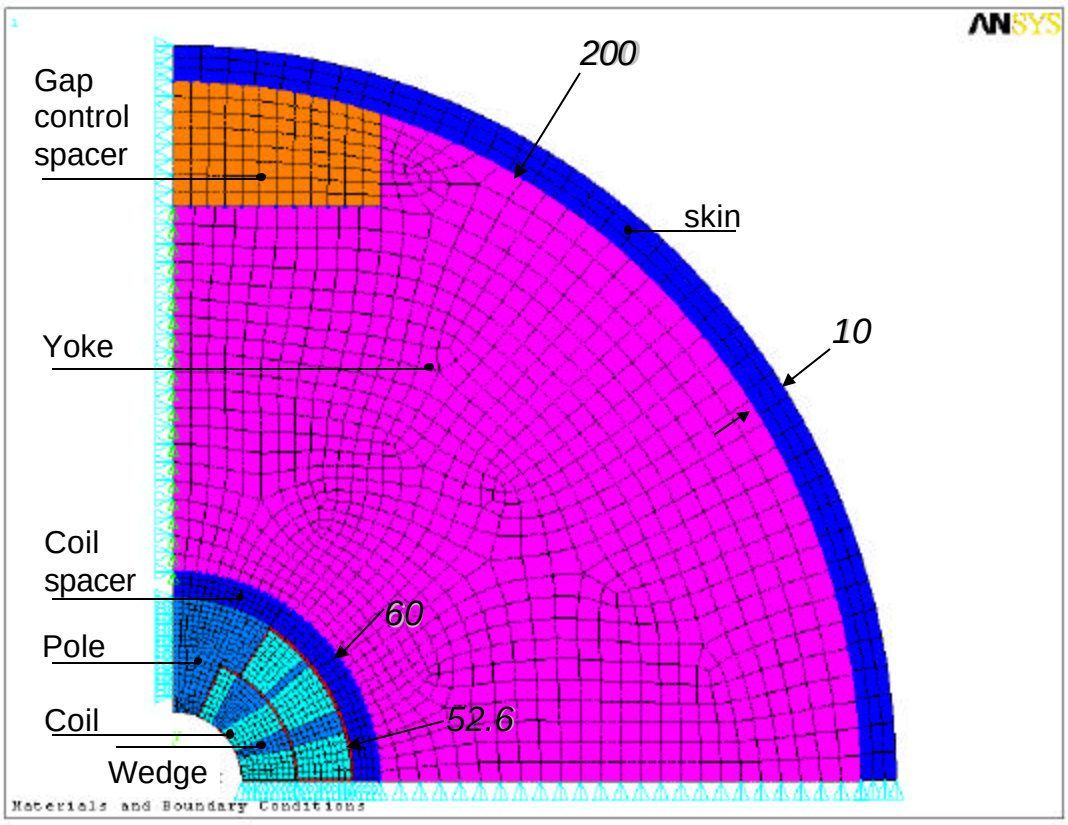

Figure 1: Cross section of the FE model.

2. MAGNETIC ANALYSIS

In order to compute the magnetic forces on the coils a finite element analysis of the cross section was performed. The main characteristics of the model used (the coils are shown in Fig. 2) are:

- A shell section represents each coil block. The sides of each shell section are two straight lines and two arcs centered in the aperture center. The edges of each bare block computed by ROXIE [5] were used to obtain the edges of these shell blocks.
- Each coil block has a uniform current distribution. The value of the current density in each block was computed to have the right overall current (i.e. the current in each cable times the number of cables in that block).
- A quadratic mesh was used in all coil blocks and wedges. Inside each inner layer block the number of elements in azimuthal direction is equal to the number of cables.
- Layer to layer and ground insulation are modeled apart from the coil layers.

The resulting forces were compared with ROXIE showing a very good agreement ($\Delta F/F < 1\%$). The Cartesian and polar components of the force at 11 T are reported in Table 3.

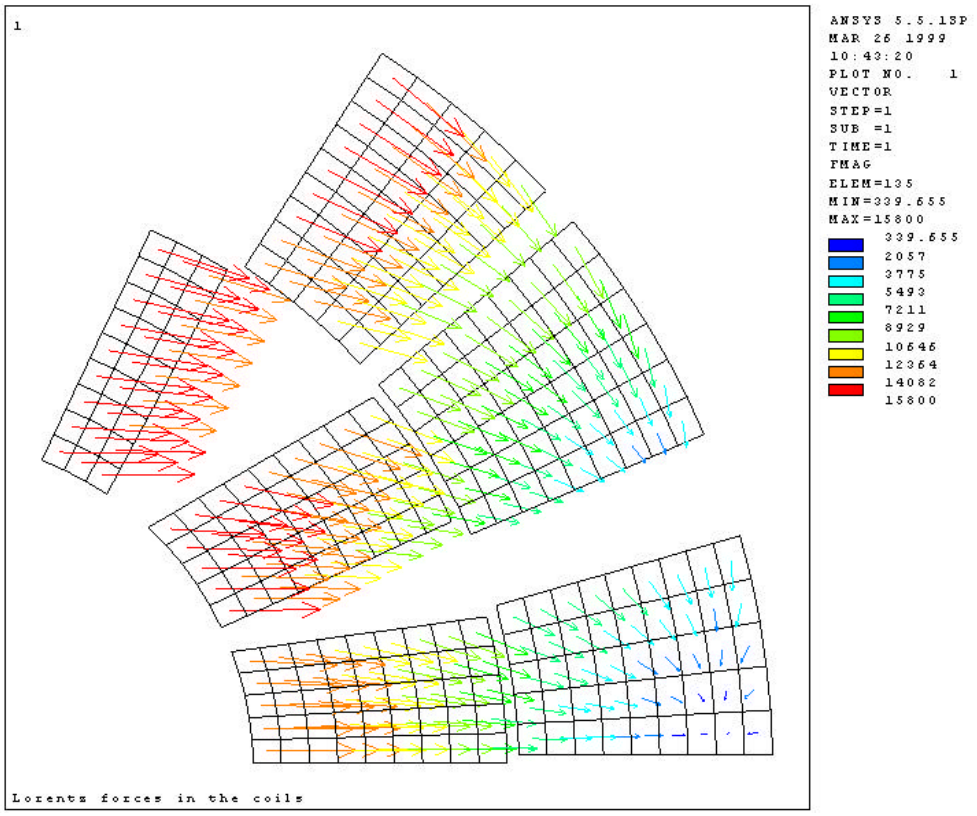

Figure 2: Detail of the cross section showing the coil and the magnetic forces.

F_x (KN/m)	2335
F_y (KN/m)	-776
F_r (KN/m)	1335
F_θ (KN/m)	-1875

Table 2: Magnetic force per quadrant @ 11 T

3. ANALYTICAL MODEL AND SIMPLE FE MODEL

An analytical model and a simple finite element model have been used to start this study before using a complex model with contact elements and all the cross section. In the analytical model coils, collars and the skin are considered as pipes with uniform and isotropic properties. The coil pipe is made of very different materials (NbSn coil and bronze pole) and the average Young modulus differs according to stress direction (i.e. whether the materials are in parallel or in series). The average of the two averages was used (E = 56 GPa). The yoke gap is always open, and the yoke is supposed to transfer the force from its outer surface to the inner always in radial direction. This model was used to compute the radial deformation of the coil pipe (ΔR_{out} = 0.035 mm) in order to have the required average prestress (σ = 60 MPa) [2]. It was also used to compute the thickness of the skin that could generate the required prestress in the coil without excessive stress in the same skin.

The simple FE model consists of the coil pipe only. It was used to apply the prestress in the coil by a uniform shrinking of the outer radius of the pipe in order to verify that the computed prestress was sufficient to keep all turns under pressure at maximum field (under the optimistic hypothesis of an infinite rigid boundary).

Both results showed that it is possible to obtain a sufficient average prestress with good distribution acting only with radial forces on the outer circumference of the coil pipe.

4. TEST MODELS

The model of all the cross section requires the use of many contact elements. They have been used between: coil pipe and coil spacers, coil spacers and yoke, yoke and skin, yoke and gap control spacer, yoke and yoke (when the gap is closed).

The errors due to the contact elements and due to the mesh in the coil pipe were evaluated by means of a simple 2D model that could be solved also analytically. The results of the comparison between the FE and the analytical model were used to choose the best kinds of contact element for this analysis and to set their properties. The error due to meshing was acceptable and no modification was done to the mesh in the coil pipe.

The test model consists of two concentric thick pipes made of different uniform and isotropic materials. The pipes are in contact without any stress at room temperature. The inner pipe has the same dimensions and the same mesh of the coil pipe. Its properties (E = 56 GPa, α = 0.99 10^{-5} 1/K) are the average of the material properties of coils and pole. The outer pipe has the same thickness of the inner one. It's made of stainless steel (E = 200 GPa) but its thermal expansion coefficient has been increased (α = 1.37 10^{-5} 1/K) to simulate the thermal contraction of all the cold mass but the coil pipe (spacers, yoke and skin).

	Radial displacement (μm)			Radial stress (MPa)			Azimuthal stress (MPa)		
	avarage	deviation	error	avarage	deviation	error	avarage	deviation	error
ANALYTIC									
Aperture	-86.7						-83.4		
Layer-layer	-131			-28.5			-54.9		
Coil outer side	-185			-35.7			-47.7		
Spacer inner side	-185			-35.7					
CONTAC48	**KN = E softer material**								
Aperture	-89.4	0.3%	3.1%				-90.3	1.3%	8.2%
Layer-layer	-134	0.1%	2.0%	-30.9	2.2%	8.4%	-59.2	0.7%	7.7%
Coil outer side	-188	0.8%	1.6%	-37.7	57.4%	5.5%	-51.6	22.7%	8.1%
Spacer inner side	-183	0.3%	-1.0%	-35.7	38.7%	0.1%			
CONTAC48	**KN = E softer material/100**								
Aperture	-66.7	0.7%	-23.1%				-26.5	4.2%	-68.2%
Layer-layer	-111	0.4%	-15.4%	-9.03	6.0%	-68.3%	-17.4	1.9%	-68.3%
Coil outer side	-162	0.4%	-12.8%	-11.4	52.2%	-68.0%	-15.4	23.6%	-67.8%
Spacer inner side	-201	0.4%	8.4%	-10.5	42.3%	-70.7%			
CONTAC52	**KN = E softer material**								
Aperture	-86.3	0.1%	-0.4%				-81.6	0.4%	-2.2%
Layer-layer	-130	0.1%	-0.5%	-27.7	0.6%	-2.8%	53.6	0.1%	-2.4%
Coil outer side	-185	0.1%	-0.4%	-34.9	10.2%	-2.2%	-46.7	3.3%	-2.2%
Spacer inner side	-186	0.1%	0.4%	-32.4	7.6%	-9.1%			
CONTAC12	**KN = E softer material/10**								
Aperture	-81.0	0.7%	-6.6%				-66.8	2.0%	-20.0%
Layer-layer	-125	0.4%	-4.7%	-22.6	2.7%	-20.8%	43.8	0.8%	-20.3%
Coil outer side	-178	0.1%	-3.7%	-28.8	10.2%	-19.3%	-38.5	3.3%	-19.4%
Spacer inner side	-190	0.1%	2.4%	-26.7	7.6%	-25.2%			

Table 3: Comparison between the analytic results and ANSYS runs with different contact elements and contact stiffness.

The model consists of about 1500 Plane42 elements and 38 contact elements. Three kinds of contact elements (Contac48, Contac12 and Contac52) have been tested using different values of the contact stiffness "KN" (in $ANSYS_{5.3}$ manual the use of a stiffness in the range from 100 to 0.01 times the stiffness of the softest contact material is suggested). Displacements and stresses (both radial and azimuthal) have been compared along 4 paths: coil pipe inner circumference, outer circumference of the first layer, coil pipe outer circumference and coil spacer inner circumference. The results of the analytical model together with the average values, the dispersions and the errors of the results from the FE models are reported in Table 4.

The best value of the contact stiffness is equal to the modulus of the softer material (KN = E softer material). It wasn't possible to use this value with Contac12 elements because the code couldn't converge.

The best results are obtained using Contac52 elements. These are node-to-node contact elements requiring a careful meshing of both the contact surfaces. Instead Contac48 are node-to-surface contact elements. They do not require any particular attention during meshing but these results show that they can be used only if good precision is not required near the contact surface.

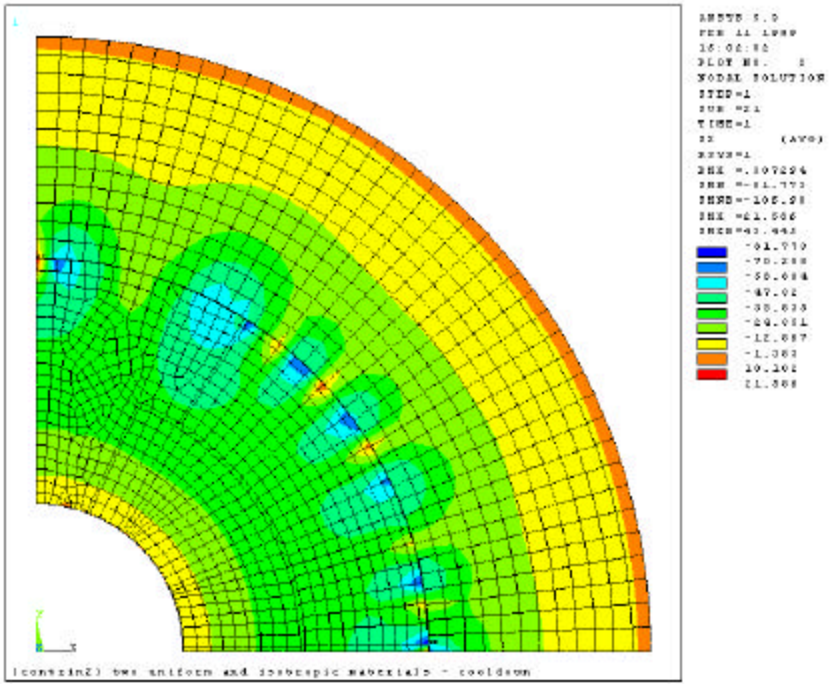

Figure 3: Radial stress in the test model using Contac48 elements with a contact stiffness (KN) equal to the Young modulus of the softer material.

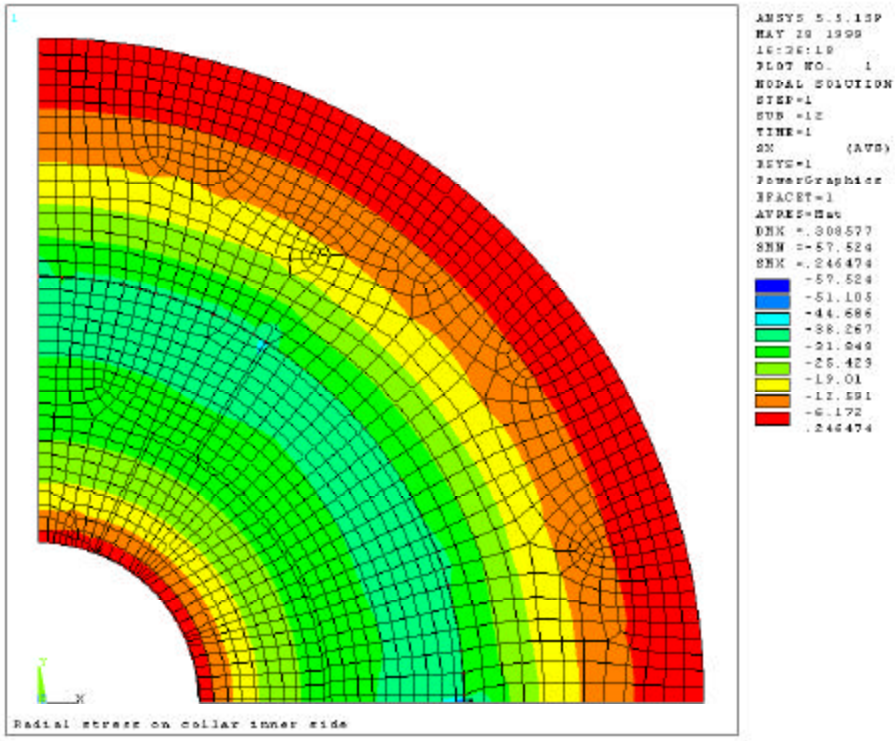

Figure 4: Radial stress in the test model using Contac52 elements with a contact stiffness (KN) equal to the Young modulus of the softer material.

In Figures 3and 4 the radial stress distribution in case of using Contac48 and contac52 elements with KN = E softer material are shown. It can be seen the uneven distribution of the force along the contact when using Contac48 elements. It is due to a different behavior of these elements according to the position of the "contact node" (on the inner surface) respect to the "target element" (on the outer surface). The force is high when the contact node is in the middle of the target element and low when it is on a side. Using Contac52 elements the dispersion is mainly due to irregular meshing and to the boundary conditions.

5. DESIGN OF THE CROSS SECTION AND FE ANALYSIS

Different solutions have been explored and many parameters have been tuned in order to find a design with the stress in coils always lower than 100 MPa. Referring to Figure 5 the main parameters studied are:

1. The stress in the skin, due to welding under pressure, that gives all prestress.
2. The dimension at room temperature of the clearance between the gap control spacer and the yoke.
3. The dimension of the tapered yoke gap. The gap should close during the cooldown and remain closed at maximum field.
4. The use and the dimension of a cut in the inner part of the pole to reduce the stress in the inner part of the coil after cooldown.

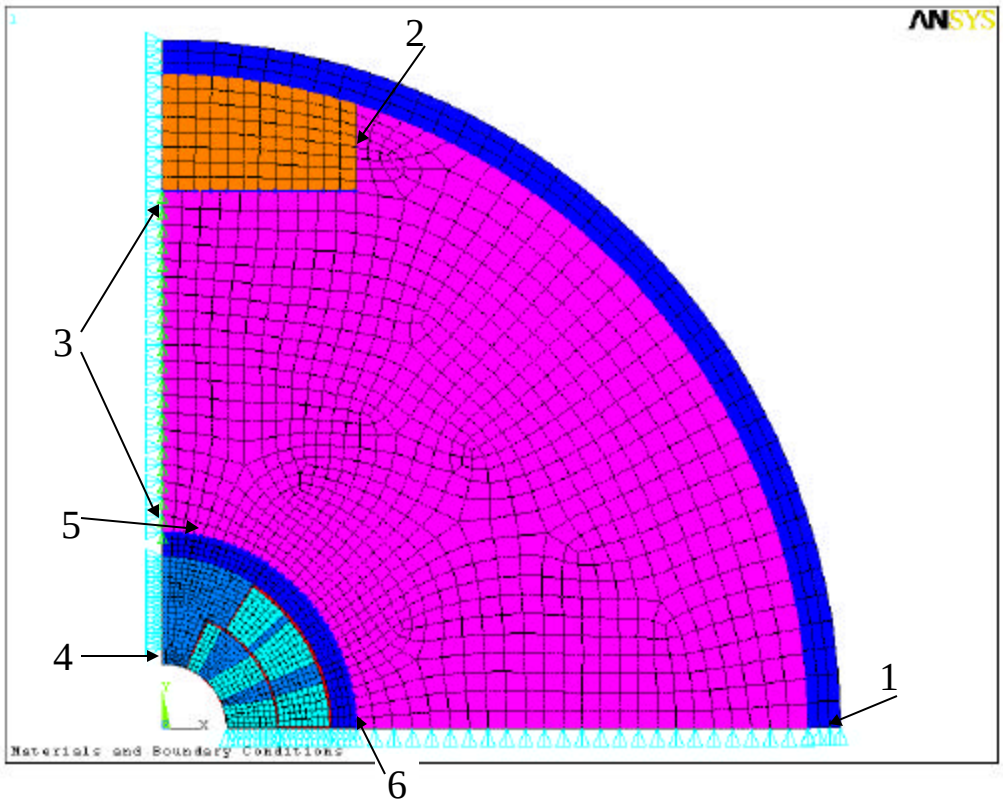

Figure 5: FE model showing the mesh, the boundary conditions and the main parameters studied.

5. The use and the dimension of shims between the coil spacers and the yoke in the area above the pole to reduce the clearance occurring at high field.
6. The use and the dimension of tapered/not-tapered shims between the coil and the coil spacers near the mid-plane to reduce the deformation of the coil at high field.

Many finite element models for the stress analysis of the cross section were done. They have been used to study different mechanical design and the influence of some parameters under all conditions: at room temperature after skin welding, at 4.2 K, at operating field (11 T) and at maximum field (12.5 T). All those models have the same mesh of the magnetic model in the coils in order to allow the automatic loading of the forces computed in the magnetic analysis. The main characteristics of these models are (see Figures 1 and 5):

- The coil pipe (coil and pole) is a unique piece made of parts with different material properties (i.e. there are no sliding surfaces between the two coil layers and between the coil and the pole because everything is glued during vacuum impregnation).
- The pole has a cut on the inner part of the symmetry plane. For simplicity it was modeled deleting the symmetry conditions on some nodes. This modeling generates a stress concentration around the end of the cut. This concentration can be reduced with a smooth shape of that region. However the aim of this model is to find the best parameters to reduce the stress in the coil. A more detailed analysis of the pole cut will be done in a second step.
- The coil spacer is made by two pieces centered on the mid-plane. No symmetry conditions are used on the vertical plane to simulate the small gap to avoid contact between the two spacers.
- Contac52 elements are used between the coil and the coil spacers. Sliding is allowed without friction. Different real constants are used for the contact elements within 8 degrees from the mid-plane in order to simulate the shims between the coil and the spacers on the mid-plane.
- The yoke has symmetry conditions on the mid-plane. The vertical gap is tapered being smaller near the coil pipe than near the gap control spacer. The closing of the gap during cooldown is modeled using a series of nodes on the vertical symmetry plane in front of the yoke edge. Symmetry conditions are applied to these nodes and each one is connected to a node of the yoke by a contact element (Contac52).
- Contac48 elements are used between the yoke and the coil spacers. Sliding is allowed without any friction. Different real constants are used along some parts of the contact surface in order to simulate the shims between the yoke and the coil spacers.
- The gap control spacer can slide without any friction both respect to the yoke and to the skin. Contac48 elements are used on the horizontal contact surface with the yoke, Contac52 elements on the vertical one. Here the gap option is used to simulate the clearance.
- The skin can slide without any friction both on the yoke and on the gap control spacer. Contac48 elements are used on both surfaces. Prestress is applied modeling the geometry with a gap between one end of the skin and the mid-plane. Tension is generated in the skin when its end is constrained to stay on the mid-plane. The dimension of the gap is used to tune the prestress.
- All contact elements have stiffness (KN) equal to the Young modulus of the softer material involved in the contact.
- All geometrical dimensions are set at room temperature without any interference or gap if not specified above.
- About 5200 elements are used. Among them there are 67 Contac52 and about 3000 Contac48 (90 contact nodes).

Dimensions and material properties used are reported in Tables 1 and 4.

Component	Material	Ther. expans. coeff.	Young Mod. @ 300 K	Young Mod. @ 4.2 K
		1/K	GPa	Gpa
Cables and insulation	Impr. Nb3Sn	$0.99\ 10^{-5}$	30	39
Coil wedges and Pole	Bronze alloy	$1.031\ 10^{-5}$	108	113
Coil spacer and Skin	Stainless steel	$1.027\ 10^{-5}$	210	225
Gap control spacer	Alluminum alloy	$1.47\ 10^{-5}$	70	81.6
Yoke	Iron	$0.7\ 10^{-5}$	210	225

Table 4: Materials and their properties

6. RESULTS

6.1 Search for the best design

In Appendix A the main results of many analyses under different conditions are reported. The data shown are:

- The azimuthal stress in 4 points of the coil: first layer top inner edge, first layer bottom inner edge, second layer top outer edge and second layer bottom outer edge.
- The radial stress in the two outer edges of the second layer.
- The force between the two halves of the yoke.
- The force between the yoke and the gap control spacer.
- The radial force between the coil spacer and the coil pipe (in three parts).
- The deformation of the coil pipe (difference between the inner radius of the coil pipe computed on the horizontal and on the vertical plane).
- The deformation of the coil spacer (same as for the coil pipe).
- The number of the closed contact elements along the yoke gap.
- The number of the open contact elements over the pole.

The last rows show the value of the main parameters used in each analysis:

- The dimension of the skin gap used to apply prestress (half gap reported).
- The dimension of the clearance (on each side) between the gap control spacer and the yoke.
- The dimensions of the tapered yoke gap (all gap at inner and outer radius).
- The interference between the coil spacer and the yoke (thickness and extension for a stepped interference, maximum thickness and overall extension for a tapered one).
- The interference between the coil pipe and the coil spacer (thickness and extension for a stepped interference, maximum thickness and overall extension for a tapered one).
- The extension of the cut in the pole along the symmetry plane.

The comparison of these results shows that:

- The difference between the maximum and the minimum azimuthal stress in the coil at operating field is almost proportional to the deformation of the coil aperture.
- In order to reduce this deformation at 11 T:
  - the yoke gap should close during cooldown and should remain closed at maximum field,
  - an opposite ('negative') deformation of the coil should be obtained after cooldown,
- A negative deformation of the coil after cooldown increases the stress on the top of the inner layer.

- A cut in the pole along the vertical plane is necessary to hallow a useful deformation after cooldown keeping the stress in the coil within an acceptable range.

6.2 Final design

During the development of these analyses we measured the Young modulus of a stack of reacted and impregnated cables with the dimensions and insulation foreseen for the magnet [6]. The measured values (E = 38 GPa both at 300 K and at 4.2 K) were used for the last two designs taking into account also different values of coil thermal contraction ($\Delta L/L$=2.9/1000 and 3.3/1000). Copper wedges and pole were used (α = 1.128 10^{-5} 1/K, E = 120 GPa @300K, 150 GPa @4.2K). Parameters and results are summarized in Table 5.

	units	300 K	4.2 K	11 T	12.5 T	300 K	4.2 K	11 T	12.5 T
Azimuthal stress									
coil top, inner edge	MPa	-77	-95	-20	3	-66	-112	-34	-4
coil top, outer edge	MPa	-50	-41	-23	-22	-50	-46	-27	-19
midplane, inner edge	MPa	-74	-28	-85	-103	-85	-47	-103	-120
midplane, outer edge	MPa	-66	-68	-81	-90	-60	-79	-90	-88
Radial stress									
coil top, outer edge	MPa	-37	-44	-35	-32	-33	-43	-33	-27
midplane, outer edge	MPa	-53	-53	-90	-106	-51	-58	-94	-102
Equivalent stress									
skin	MPa	243	389	389	390	270	396	398	401
Force/length									
yoke-yoke	KN/m	0	-1551	-751	-524	0	-798	0	0
yoke-gap control spacer	KN/m	0	0	0	0	-377	-460	-543	-495
yoke-coil spacer 0-8 deg	KN/m	-347	-343	-579	-650	-332	-379	-603	-651
5-65 deg	KN/m	-2232	-2237	-2927	-3115	-2071	-2596	-3207	-3240
65-90 deg	KN/m	-941	-560	-225	-139	-1028	-707	-346	-230
Deformation = R_midplane - R_pole									
aperture	µm	-28	-64	3	25	-11	-61	8	34
(filename)		(newmatA1)				(highthc1)			
Parameters									
Coil $\Delta L/L$ 300K-4.2K		2.9/1000				3.3/1000			
welding Dl	mm	0.4				0.4			
gap cont. sp. clearance	mm	0.1				0.01			
yoke inner gap	mm	0.22				0.22			
yoke outer gap	mm	0.32				0.32			
coil sp.-yoke interf.	µm	0				23	MAX		
coil sp.-yoke int. arc	deg.					0-90	Tapered interference		
coil-coil sp. interf.	µm	0				0			
coil-coil sp. int. arc	deg.								
cut in pole wedge	mm	4				4			

Table 5: Parameters and results of the last designs. See text for details.

These solutions are quite different because in the second model an interference between coil spacer and yoke is used to compensate the higher thermal contraction, and the gap control spacer is used to reduce the prestress at room temperature. Using these parameters the yoke closes during cooldown but the gap is open at operating field. Because of this the coil deformation at maximum field is bigger than in the first solution and therefore also the difference between the minimum

and the maximum stress is higher. This solution can be optimized but it is useful to show that this mechanical design can be used in a large range of values of the coil thermal contraction coefficient.

In Figures 6 to 9 the azimuthal stress in the coil of the second model (ΔL/L= 3.3/1000) is shown in all conditions. In Figures 10 and 11 it can be seen the radial stress in the coil pipe after cooldown and at 11 tesla. The undeformed shape (solid line) and the nodal forces (forces applied from the selected part of the model to the other parts and boundaries) are also shown. The cut in the pole along the vertical plane reduces the azimuthal stress in the inner layer after cooldown but could increase the shear stress in the coil. In Figure 12 it can be seen that the shear stress in the coil after cooldown doesn't exceed 12 MPa.

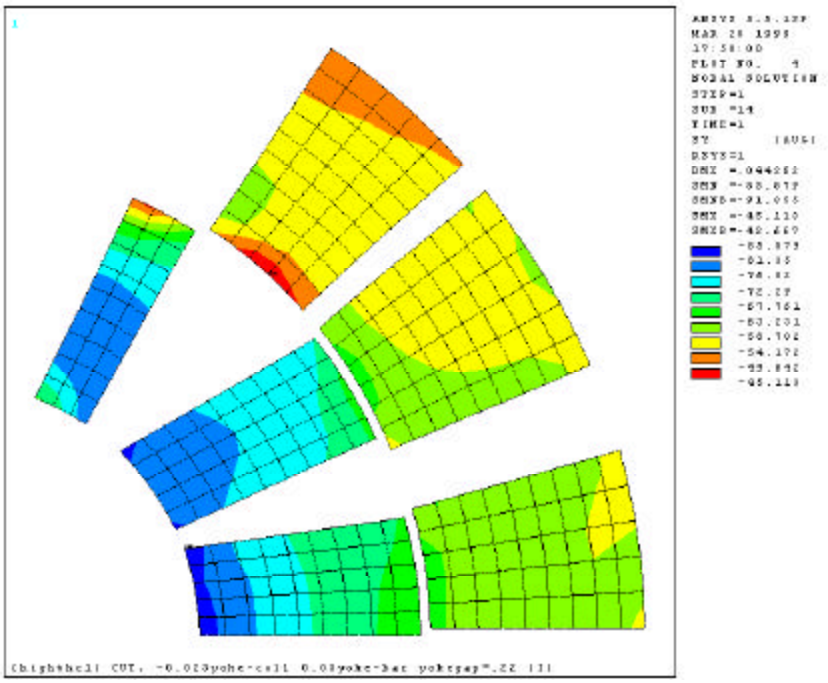

Figure 6: Azimuthal stress in the coil at room temperature after assembling

7. CONCLUSIONS

According to these results it can be said that a mechanical design with only thin spacers between the coil pipe and the yoke (i.e. without collars), with a yoke gap open at room temperature but always closed at 4.2K, and with prestress applied only by the skin (welded under a press) is feasible. The stress in the coil is always acceptable and all parts of the coil keep a good prestress in operating condition. The coil deformation at high field is very small because an opposite deformation is generated during the cooldown. The cut in the pole allows this deformation during cooling down without excessive stress in the coil.

The last results have shown that this mechanical design can be used for coils with different thermal contraction coefficient with small changes of interferences.

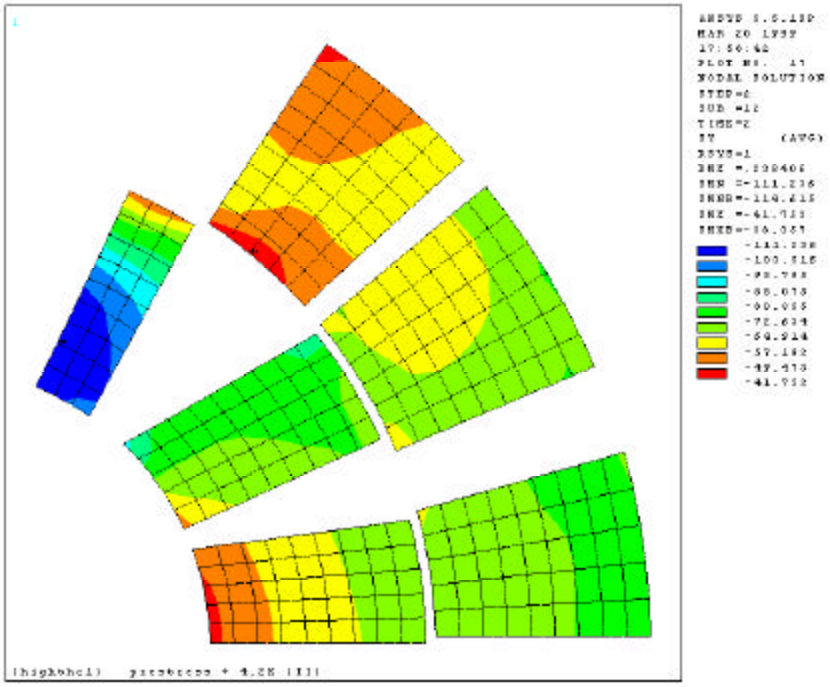

Figure 7: Azimuthal stress in the coil after cooldown. ΔL/L = 3.3/1000

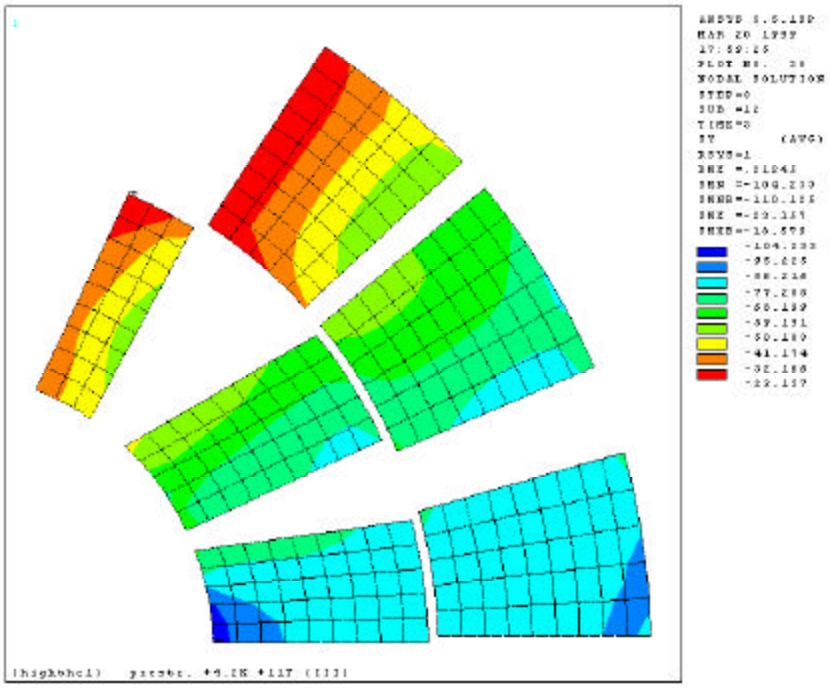

Figure 8: Azimuthal stress in the coil at 11T.

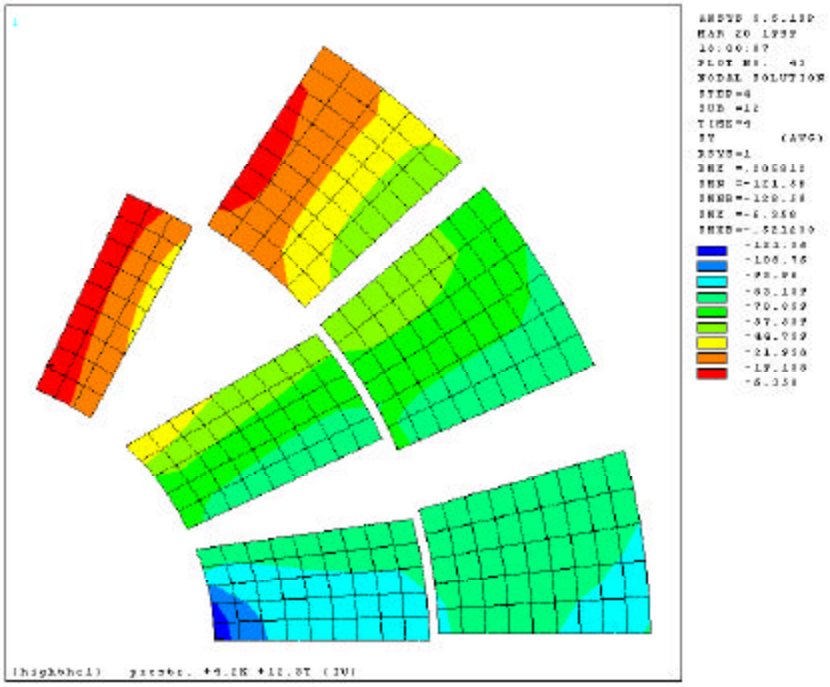

Figure 9: Azimuthal stress in the coil at 12.5 T.

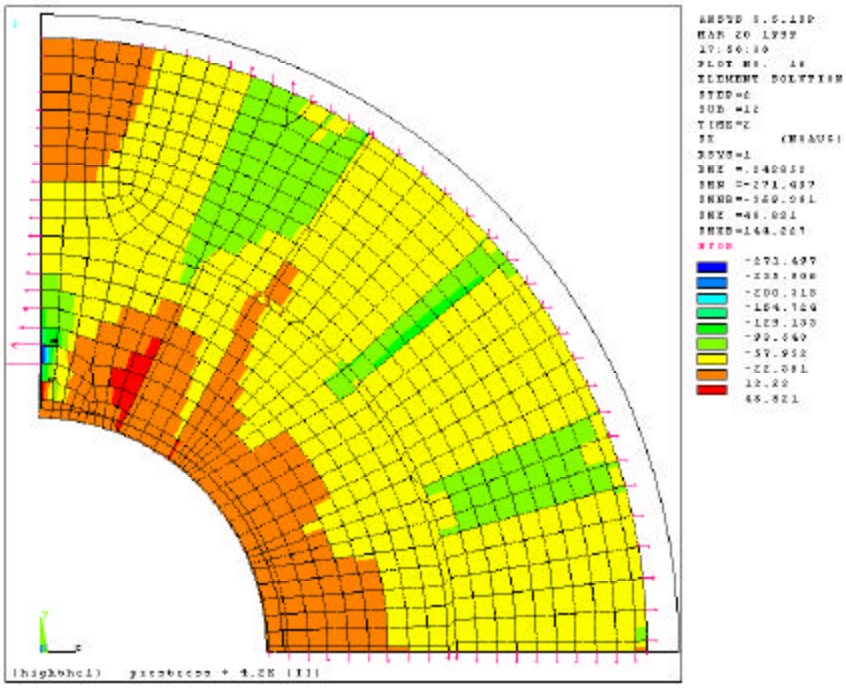

Figure 10: Radial stress in the coil pipe after cooldown. Nodal forces and undeformed shape also shown.

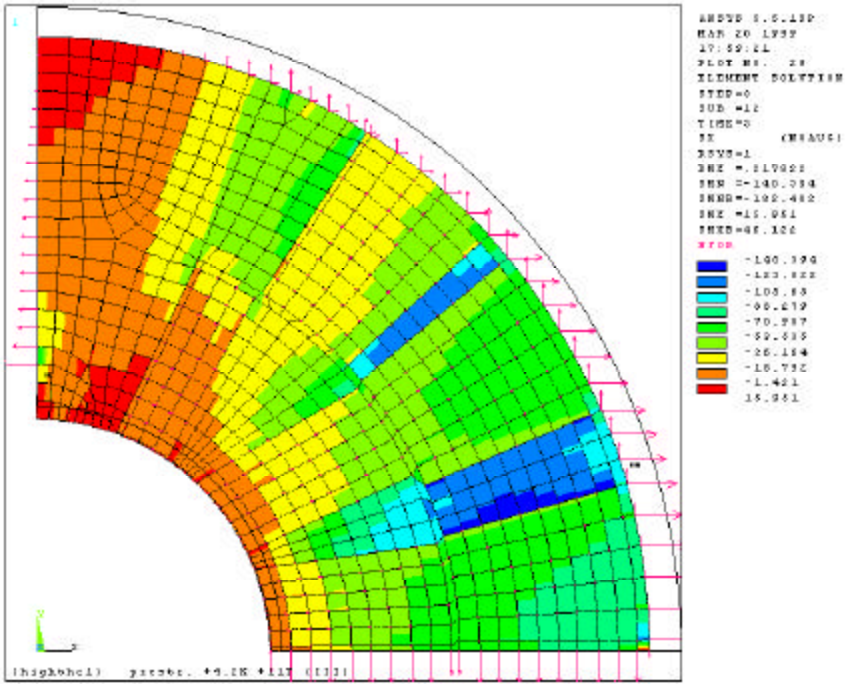

Figure 11: Radial stress in the coil pipe at 11 T. Nodal forces and undeformed shape also shown.

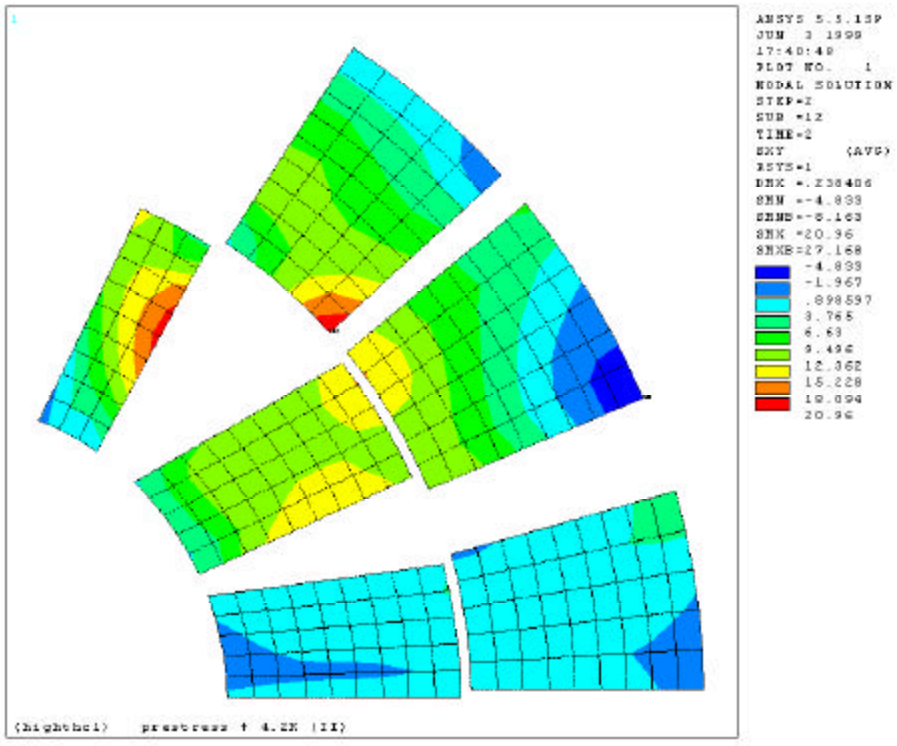

Figure 12: Shear stress in the coil after cooldown.

REFERENCE

[1] S. Caspi, M. Wake *"A 12 tesla dipole for the VLHC"* SC-MAG-635, LBL, December 1998.
[2] V.V. Kashikhin, I. Terechkine "40-mm bore dipole cross-section using cable made of 1-mm-diameter NbSn strand" TD-99-014, FNAL, May 1999.
[3] G. Ambrosio, V.V. Kashikhin "40-mm bore HFM cross section design with 0.8 mm strand diameter NbSn cable" TD-99-010, FNAL, May 1999.
[4] R. Yamada, J. Moeller, M. Wake "Design study of 45-mm bore dipole magnet for 11 to 12 tesla field" TD-99-012, FNAL, March 1999.
[5] S. Russenchuck "A computer program for the design of superconducting accelerator magnets" AT/95-39, LHC note 354, CERN, September 1995.
[6] D.R. Chichili, T.T. Arkan, I. Terechkine "Niobium-Tin magnet technology development at Fermilab" CONF-99-052, FNAL, 1999.

APPENDIX: parameters and results of some models used during the development of the design. See text for details.

	units	300 K	4.2 K	11 T	300 K	4.2 K	11 T	300 K	4.2 K	11 T
Azimuthal stress (radial stress)										
coil top, inner edge	MPa	-95	-183	-42	-93	-146	-32	-66	-144	-7
coil top, outer edge	MPa	-36 (-5)	-49 (-31)	-25 (-10)	-35 (-1)	-36 (-3)	-22 (-1)	-29 (-2)	-33 (-0.5)	-15 (-3)
midplane, inner edge	MPa	-86	-73	-132	-88	-71	-132	-78	-63	-122
midplane, outer edge	MPa	-60 (-47)	-97 (-70)	-90 (-91)	-64 (-57)	-85 (-72)	-96 (-109)	-51 (-47)	-83 (-69)	-84 (-99)
MAX (if not at edges)										
skin	MPa									
Force/length										
yoke-yoke	KN/m	0	-157	0	0	-872	-97	0	-382	0
yoke-gap ct. sp.	KN/m	0	0	0	0	0	0	0	0	0
pole-coil spacer	KN/m	-1410	-1528	-1076	-1471	-1485	-1116	-1285	-1400	-938
all coil+pole - coil spacer	KN/m									
Deformation = R_midplane - R_pole										
aperture	μm	0	-51	28	3	-32	33	12	-35	39
coil sp. inner side	μm	-51	-104	-46	-49	-85	-42	-37	-88	-33
Contact										
yoke - yoke	closed	0	2	0	0	9	7	0	5	0
over the pole	open	0	1	2	0	1	2	0	1	3
(filname)		(mechqua2.db)			(mechqua3.db)			(mechqua4.db)		
Parameters										
welding Dl	mm	0.4			0.4			0.3		
gap contr. sp. clearence	mm	0.1			0.1			0.1		
yoke inner gap	mm	0.3			0.25			0.25		
yoke outer gap	mm	0.5			0.35			0.35		
coil sp.-yoke interference	μm	35			35			35		
coil sp.-yoke interf. ext.	deg.	65-90			65-90			65-90		

	units	300 K	4.2 K	11 T	300 K	4.2 K	11 T	300 K	4.2 K	11 T
Azimuthal stress (radial stress)										
coil top, inner edge	MPa	-93	-108	6	-99	-138	-29	-99	-98	11
coil top, outer edge	MPa	-35 (-1)	-29 (-2)	-15 (-3)	-55 (-36)	-58 (-48)	-42 (-40)	-55 (-36)	-47 (-36)	-30 (-28)
midplane, inner edge	MPa	-88	-66	-126	-101	-85	-141	-101	-76	-132
midplane, outer edge	MPa	-64 (-57)	-67 (-59)	-79 (-96)	-58 (-48)	-72 (-56)	-85 (-94)	-58 (-48)	-53 (-42)	-66 (-80)
MAX (if not at edges)		-95								
skin	MPa									
Force/length										
yoke-yoke	KN/m	0	-1560	-792	0	-1136	-337	0	-1900	-1104
yoke-gap ct. sp.	KN/m	0	0	0	0	0	0	0	0	0
pole-coil spacer	KN/m	-1472	-1320	-941						
all coil+pole - coil spacer	KN/m				-3710	-4082	-4648	-3709	-3223	-3778
Deformation = R_midplane - R_pole										
aperture	µm	3	-17	47	7	-23	37	6	-9	51
coil sp. inner side	µm	-49	-66	-23	-4	-35	5	-4	-14	25
Contact										
yoke - yoke	closed	0	12	16	0	2-12	5-15	0	2-15	2-19
over the pole	open	0	1	2	0	1	1	0	1	1
(filname)		(mechqua5.db)			(mechpen1.db)			(mechpen2.db)		
Parameters										
welding Dl	mm	0.4			0.4			0.4		
gap contr. sp. clearence	mm	0.1			0.1			0.1		
yoke inner gap	mm	0.2			0.2			0.15		
yoke outer gap	mm	0.3			0.3			0.25		
coil sp.-yoke interference	µm	35			35	MAX		35	MAX	
coil sp.-yoke interf. ext.	deg.	65-90			0-90	Tapered interference		0-90	Tapered interference	

	units	300 K	4.2 K	11 T	300 K	4.2 K	11 T	300 K	4.2 K	11 T
Azimuthal stress (radial stress)										
coil top, inner edge	MPa	-100	-104	5	-104	-118	-8	-102	-112	-3
coil top, outer edge	MPa	-54 (-36)	-48 (-37)	-31 (-29)	-54 (-35)	-49 (-38)	-31 (-29)	-54 (-35)	-48 (-38)	-32 (-30)
midplane, inner edge	MPa	-94	-69	-125	-80	-53	-110	-86	-59	-116
midplane, outer edge	MPa	-94 (-99)	-97 (-105)	-110 (-144)	-112 (-116)	-122 (-127)	-138 (-169)	-100 (-100)	-106 (-108)	-121 (-149)
skin	MPa									
Force/length										
yoke-yoke	KN/m	0	-1833	-1033				0	-1718	-938
yoke-gap cont.sp.	KN/m	0	0	0				0	0	0
coil pipe- coil sp. 0-5 deg.	KN/m	-484	-509	-671				-793	-849	-1118
coil pipe- coil sp. 5-65 deg.	KN/m	-2135	-1920	-2659				-1821	-1669	-2293
coil pipe- coil sp. 65-90 deg.	KN/m	-1114	-902	-552				-1151	-962	-608
Deformation = R_midplane - R_pole										
aperture	μm			46				-1	-20	40
collar inner side	μm							6	-8	22
Contact										
yoke - yoke	closed	0	2-15	2-19				0	2-15	2-19
over the pole	open	0	0	1				0	0	1
(filname)		(mechpen3.db)			(mechpen4.db)			(mechpen5.db)		
Parameters										
welding Dl	mm	0.4			0.4			0.4		
gap contr. sp. clearance	mm	0.1			0.1			0.1		
yoke inner gap	mm	0.15			0.15			0.15		
yoke outer gap	mm	0.25			0.25			0.25		
coil sp.-yoke interference	μm	35	MAX		35	MAX		35	MAX	
coil sp.-yoke interf. Arc	deg.	0-90	Tapered interference		0-90	Tapered interference		0-90	Tapered interference	
coil-coil sp. interf.	μm	30			60			45		
coil-coil sp. int. arc	deg.	0-5			0-8			0-8		
cut in pole wedge	mm									

	units	300 K	4.2 K	11 T	300 K	4.2 K	11 T	300 K	4.2 K	11 T
Azimuthal stress (radial stress)										
coil top, inner edge	MPa	-100	-72 *	-4	-70	-93	-26	-68	-87 *	-20
coil top, outer edge	MPa	-55 (-35)	-49 (-37)	-32 (-30)	-56 (-36)	-60 (-48)	-43 (-41)	-56 (-36)	-60 (-47)	-42 (-40)
midplane, inner edge	MPa	-86	-59	-116	-91	-73	-131	-101	-84	-141
midplane, outer edge	MPa	-100 (-100)	-106 (-106)	-121 (-149)	-88 (-84)	-108 (-100)	-121 (-139)	-59 (-48)	-71 (-54)	-85 (-94)
skin	MPa									
Force/length										
yoke-yoke	KN/m	0	-1781	-936	0	-1110	-250	0	-1219	-352
yoke-gap cont.sp.	KN/m	0	0	0	0	0	0	0	0	0
coil pipe- coil sp. 0-5 deg.	KN/m	-792	-838	-1119	-649	-763	-1008			
coil pipe- coil sp. 5-65 deg.	KN/m	-1803	-1598	-2296	-1950	-2316	-3060	-2605	-2991	-3981
coil pipe- coil sp. 65-90 deg.	KN/m	-1181	-990	-607	-1157	-1084	-720	-1116	-1019	-653
Deformation = R_midplane - R_pole										
aperture	µm	-11	-30	41	-9	-43	28	-3	-36	36
collar inner side	µm	2	-22	32	-1	-38	9			
Contact										
yoke - yoke	closed	0	2-15	2-19	0	2-12	5-14	0	2-12	4-15
over the pole	open	0	0	1	0	1	1	0	1	1
(filname)		(mechpen6.db)			(mechpen7.db)			(mechpen8.db)		
Parameters										
welding Dl	mm	0.4			0.4			0.4		
gap contr. sp. clearance	mm	0.1			0.1			0.1		
yoke inner gap	mm	0.15			0.2			0.2		
yoke outer gap	mm	0.25			0.3			0.3		
coil sp.-yoke interference	µm	35	MAX		35	MAX		35	MAX	
coil sp.-yoke interf. Arc	deg.	0-90	Tapered interference		0-90	Tapered interference		0-90	Tapered interference	
coil-coil sp. interf.	µm	45			30			0		
coil-coil sp. int. arc	deg.	0-8			0-8					
cut in pole wedge	mm	4			4			4		

	units	300 K	4.2 K	11 T	300 K	4.2 K	11 T	300 K	4.2 K	11 T	12.5 T
Azimuthal stress (radial)											
coil top, inner edge	MPa	-80	-95 *	-28	-79	-94 *	-27	-79	-92	-25	-4
coil top, outer edge	MPa	-47 (-35)	-47 (-43)	-36 (-29)	-47 (-35)	-47 (-43)	-28 (-35)	-47 (-35)	-46 (-42)	-28 (-35)	-22 (-32)
midplane, inner edge	MPa	-64	-37	-94	-67	-40	-97	-69	-43	-100.6	-118
midplane, outer edge	MPa	-85 (-79)	-100 (-91)	-113 (-130)	-75 (-65)	-87 (-73)	-100 (-112)	-64 (-50)	-73 (-55)	-87 (-94)	-90 (-106)
skin	MPa							236	389	390	390
Force/length											
yoke-yoke	KN/m	0	-1368	-519	0	-1395	-547	0	-1424	-577	-345
yoke-gap cont.sp.	KN/m	0	0	0	0	0	0	0	0	0	0
coil pipe-sp. 0-8 deg.	KN/m	-497	-560	-807	-413	-457	-704	-329	-354	-601	-673
coil pipe-sp. 5-65 deg.	KN/m	-2009	-2185	-2924	-2095	-2264	-3004	-2180	-2343	-3084	-3282
coil pipe-sp. 65-90 deg.	KN/m	-890	-735	-379	-878	-717	-362	-867	-699	-345	-244
Deformation = R_midplane - R_pole											
aperture	μm	-37	-65	5	-36	-63	7	-34	-61	10	33
collar inner side	μm							-43	-68	-26	-11
Contact											
yoke - yoke	closed		2-14	5-19		2-15	5-19		2-15	5-19	8-20
over the pole	open	1	2	5	1	3	5	1	3	5	6
(filname)		(mechses1.db)			(mechses2.db)			(mechses3.db)			
Parameters											
welding Dl	mm	0.4			0.4			0.4			
gap contr. sp. clearance	mm	0.1			0.1			0.1			
yoke inner gap	mm	0.22			0.22			0.22			
yoke outer gap	mm	0.32			0.32			0.32			
coil sp.-yoke interf. arc	μm	0	NO collar-yoke interf.		0	NO collar-yoke interf.		0	NO collar-yoke interf.		
coil sp.-yoke interf. arc	deg.										
coil-coil sp. interf.	μm	20	MAX		10	MAX		0	NO coil-collar interferen.		
coil-coil sp. int. arc	deg.	0-5-8	Tapered interference		0-5-8	Tapered interference					
cut in pole wedge	mm	4			4			4			